J. Phys. Chem. A **2000,** *104,* 5503−5510

Kinetics of Cl Atom Reactions with C_2H_5Cl and C_2H_4Cl Radical and the Disproportionation of $2C_2H_4Cl$ at 298 K and at Millitorr Pressures

Otto Dobis and Sidney W. Benson*

Loker Hydrocarbon Research Institute, University of Southern California, University Park, Los Angeles, California 90089-1661

Received: September 8, 1999; In Final Form: March 21, 2000

The bimolecular reaction $Cl + C_2H_5Cl \rightarrow HCl + C_2H_4Cl$ (1) is studied in the very-low-pressure reactor (VLPR) system at room temperature. Detailed mass spectrometric analysis of simultaneous reactant consumption and product formation rates indicates that the overall mechanism also includes two disproportionation reactions: $Cl + C_2H_4Cl \rightarrow HCl + C_2H_3Cl$ (2) and $2C_2H_4Cl \rightarrow C_2H_5Cl + C_2H_3Cl$ (3). Rate constants obtained for these reactions are: $k_1 = (8.07 \pm 0.36) \times 10^{-12}$, $k_2 = (1.18 \pm 0.06) \times 10^{-11}$, and $k_3 = (1.83 \pm 0.15) \times 10^{-12}$ cm^3/(molecule-s). The decrease in the reactivity of C_2H_5Cl compared with C_2H_6 reactivity in reaction type (1) correlates well with the electronegativity of the Cl substituent. The decrease points to a dipole−dipole repulsion in the transition state. Preliminary measurement of the reaction of C_2H_4Cl radical with Cl_2 yields a value of $k_5 = (1.7 \pm 1.0) \times 10^{-13}$ cm^3/(molecule-s).

Introduction

The reaction of chlorinated hydrocarbons with the Cl atom is an important elementary step of a number of complex processes, such as the polychlorination of hydrocarbons and the incineration of hazardous, halogen-containing organic materials. To model and design both multistep processes on an industrial scale requires well-known rate constants and thermochemical quantities for each elementary step as input data.

The importance of the reaction

$$Cl + C_2H_5Cl \rightarrow HCl + C_2H_4Cl + 5.7\ \text{kcal/mol} \qquad (1)$$

is that it contributes to a secondary chain propagation step in the thermal- or photochlorination of $C_2H_6 + Cl_2$. The disproportionation steps

$$Cl + C_2H_4Cl \rightarrow HCl + C_2H_3Cl \qquad (2)$$

and

$$2C_2H_4Cl \rightarrow C_2H_5Cl + C_2H_3Cl \qquad (3)$$

may also contribute to termination in the above chain chlorination process.

Competitive photochlorination studies simplify kinetic studies to a relative rate measurement[1] that can then give the rate constant k_1 relative to a well-known rate constant of a selected reference reaction. However, to achieve an accurate relative rate measurement, the competitive reaction system must satisfy several conditions,[1,6,7] such as low conversions to minimize complications from secondary reactions and long chain lengths, so that termination products can be neglected. To illustrate just the importance of the reference reaction choice, let us examine some kinetic data on reaction 1 derived from competitive measurements.

An early competitive photochlorination study of the C_2H_5Cl/C_2H_6 system[2] with measurement of both reactants and products reported $k_1/k_{ref} = 0.167 \pm 0.024$ at room temperature. Using the updated[3] $k_{ref} = (6.1 \pm 0.1) \times 10^{-11}$ cm^3/(molecule-s) for the $Cl + C_2H_6$ reference reaction, $k_1 = (10.2 \pm 1.5) \times 10^{-12}$ cm^3/(molecule-s) is obtained. A similar competitive rate measurement[4] using the same C_2H_6 standard, but using infrared (IR) absorption spectral analysis of reactant consumption, gives $k_1 = (11.6 \pm 1.6) \times 10^{-12}$ cm^3/(molecule-s), which is in good agreement. However, the authors of the latter result reported in a follow-up publication[5] that the value may be anomalously high and gave a new value of $k_1 = (8.7 \pm 1.0) \times 10^{-12}$ cm^3/(molecule-s), remeasured in the same competitive system.

Photochlorination of C_2H_5Cl/CH_4 mixtures in a competitive reaction system[6] using gas chromatographic (GC) analysis of chlorinated product yields ($C_2H_4Cl_2$ and CH_3Cl) and gives $k_1 = (3.75 \pm 0.53) \times 10^{-12}$ cm^3/(molecule-s) at room temperature. In two subsequent papers,[7] the authors report $k_1 = (7.12 \pm 0.14) \times 10^{-12}$ cm^3/(molecule-s) using a GC detector sensitivity for CH_3Cl that was increased by a factor of 2 relative to their former work.[6] From a combination of three different relative rate measurements,[8] a rate constant ratio of k_1 relative to $Cl + CH_4$ reference reaction can also be derived, which then leads to an approximate value of $k_1 \sim 9.2 \times 10^{-12}$ cm^3/(molecule-s) at 298 K. Although both reference rate constants have well-established values,[3,9] the values of k_1 derived from these relative measurements vary by a factor of 1.6.

Another example of relative rate measurements[10] is provided by the photobromination of the two reactants C_2H_5Cl and C_2H_6. In contrast to the photochlorination study of this pair just mentioned, the first and slowest step in the photobromination chain is the endothermic abstraction of an H atom by a Br atom. The analogous $Cl + C_2H_6$ reaction is exothermic. The bromination study has been used to establish values of the bond dissociation energies of both the α-C−H and β-C−H bonds of C_2H_5Cl.

An absolute rate measurement has been carried out by laser flash photolysis of Cl_2 followed by time-resolved resonance fluorescence spectrometry of Cl signal decay in reaction 1 under pseudo-first-order conditions for C_2H_5Cl concentration,[11] with special care to reduce the kinetic interference of consecutive reactions. The reported[11] value is $k_1 = (8.04 \pm 0.57) \times 10^{-12}$

10.1021/jp993163m CCC: $19.00 © 2000 American Chemical Society
Published on Web 05/17/2000

cm^3/(molecule-s) at room temperature. Another flash photolysis system comprising reaction 1 and

$$C_2H_4Cl + O_2 \rightarrow C_2H_4ClO_2 \quad (4)$$

$$C_2H_4Cl + Cl_2 \rightarrow C_2H_4Cl_2 + Cl \quad (5)$$

consecutive competitive reactions using time-resolved IR spectrometry of HCl formation gave[12] $k_1 = (6.8 \pm 1.4) \times 10^{-12}$ and $(7.5 \pm 0.6) \times 10^{-12}$ cm^3/(molecule-s) in separate sets of experiments.[13] This system is not a conventional flash system for absolute rate constant measurement because the reported exponential growth of HCl product also depends on the $k_5[Cl_2]/k_4[O_2]$ ratio, and the time delay must be long enough to reach the steady-state value of $[C_2H_4Cl]$ radical concentration. The authors[12] treated the measured HCl data with a single exponential growth curve when rigorously it should be treated as a double exponential growth curve. They assumed that the radical concentration was in steady state relative to Cl atom concentration, an assumption that is only valid after several half-lives of the initial $[Cl]_o$ have elapsed. In principle, the ratio k_5/k_4 should be pressure dependent. Its value is determined from both the GC analysis and IR absorption spectrometry of products as $k_5/k_4 = 0.42 \pm 0.06$ for α-chloroethyl and 0.63 ± 0.15 for β-chloroethyl radicals at 700 Torr pressure.[12] With the α/β chloroethyl radical distribution given later, this rate constant ratio is 0.46 ± 0.08. Using the assumption of Kaiser et al.[12] that $k_4 = 9 \times 10^{-12}$ cm^3/(molecule-s), the same as for the $C_2H_5 + O_2$ reaction,[14] $k_5 = 4.2 \times 10^{-12}$ is obtained. This result is in excellent agreement with the value of $k_5 = (4.37 \pm 0.69) \times 10^{-12}$ cm^3/(molecule-s) derived from direct photolysis/photoionization mass spectrometry (MS) measurements.[15] However, this result is ~2 orders of magnitude higher than what was estimated for it as a side reaction in the direct flash system[11] used for the kinetic study of reaction 1. In a Cl_2-rich system, the chain recovery of Cl by reaction 5 would reduce the measured Cl consumption rate, although no such effect was observed when a $[O_2]/[Cl_2]$ ratio of ~250 was used for control measurements[11] at 100 Torr overall pressure. In contrast, the $[O_2]/[Cl_2]$ ratio was varied between 2 and 10 in the former[12] flash system. The absolute rate constant measurements just presented show good agreement in k_1 values, but with some unexplained inconsistency in the rate of side reaction 5 that we will return to later.

The H atoms in the $-CH_2$ group of CH_3CH_2Cl are about four times more reactive in reaction 1 than those of the $-CH_3$ group. The two isomers of the C_2H_4Cl radical cannot be measured separately by our MS analysis, but the isomeric radical ratio is measured in a number of studies by secondary product analysis.[5−7,12,13] Regardless of the absolute values of k_1, they report the CH_3CHCl radical at 81 to 83% of total radical formation, with a good average of 82%. This radical isomer distribution was taken into account when calculating the exothermicity of reaction 1.

The inconsistencies in the kinetic measurements of reaction 1 call for further investigation of this subject by alternative methods. Our very-low-pressure reactor (VLPR) system is well suited to carry out this task by measuring the rate of reaction 1 under steady-state conditions that, in turn, also allows the kinetic study of both reactions 2 and 3.

Experimental Section

The VLPR system used for the current kinetic investigation is the same[3,9,16] three-stage system with all turbo-pumped equipment we have used for all previous studies. It has been described in detail earlier.[9] The experimental sequence, the system parameters, and MS analysis used for data processing are briefly summarized below.

The fundamental part of the system is the thin-Teflon-coated, cylindrical, thermostated flow cell reactor of volume $V_r = 217.5$ cm^3 mounted on the top of the main vacuum chamber. Gas inlets are affixed on the top of this reactor and preceded by resistive capillary flow subsystems calibrated for regulating the fluxes of initial gas components with the use of Validyne transducers. One of the inlets is connected through a phosphoric acid-coated quartz discharge tube centered in the Opthos microwave generator cavity of a McCarrol antenna before joining at the tapered capillary inlet of the reactor cell. This feed-through is used for a 5% Cl_2/He gas mixture flow to provide the initial Cl concentration in the reactor when running the microwave generator. A second inlet is used for a 4.8% C_2H_5Cl/He gas mixture flow that provides the initial C_2H_5Cl reactant concentration for reaction 1 in the reactor.

The gas mixture leaves at the bottom of the reactor through an escape orifice of 0.277 cm diameter (marked ϕ_3 in our earlier studies[3,9,16]) in the form of an effusive molecular beam. This beam is chopped by a tuning fork and further collimated by two successive pinholes in the differentially pumped vacuum system to reduce the background signal. The beam is sampled with the off-axis mass analyzer of the mass spectrometer, and the mass signals are fed to a phase-sensitive lock-in amplifier tuned to the chopping frequency. The measured mass ranges are repeatedly scanned, usually 20−30 times, to give a good statistical average, and the mass intensities are recorded for data acquisition. Each mass signal is corrected for its small background value recorded prior to the start-up of mass flow. The chopping and phase-sensitive detection ensures that we are sampling species that have not made collisions after leaving the reactor.

With the reactor volume V_r and orifice size just described, the first-order escape rate constant for any gas component of mass M is given by $k_{eM} = 0.546(T/M)^{1/2}$ s^{-1}, where T is in degrees Kelvin. The strictly controlled gas inlet and outlet dynamics establish the well-defined steady-state flow conditions in the reactor, which operates in the Knudsen flow regime.

In addition to the mass analysis of Cl, Cl_2, and HCl, there are three chlorocarbon compounds with considerable fragment interference in their spectra. The resolution of those spectra is a fundamental and essential part of our kinetic investigation.

Mass spectral calibration for a given gas component of mass M is carried out by measuring the mass signal intensity I_M as a function of the specific flux $F(M)$ according to the relationship $I_M = \alpha_M F(M)$, where α_M is the mass spectral efficiency for mass M and $F(M)$ = flux/V_r in units of molecules/(cm^3-s). This relationship is strictly linear in the mass flow range used as is shown in Figures 1 and 3. The steady-state concentration of the gas component M in the reactor cell can then be calculated from the relation $[M] = F(M)/k_{eM}$.

Our mass spectrometer is very sensitive to halogenated species including ethyl chloride (RCl) as shown in Figure 1, where the cross-section efficiencies (α_Σ) are $(3.528 \pm 0.082) \times 10^{-10}$ with 40 V and $(1.01 \pm 0.02) \times 10^{-10}$ with 20 V ionization energies. The total ion yield ΣI_x incorporates the contribution of a large amount of fragmentation of the parent molecule even at low ionization voltages. These fragments can be assembled into three groups according to the three possible types of initial break-up of the molecule. The electron energy dependence of these group contributions is shown in Figure 2. The group distributions (in percentage) at the two electron

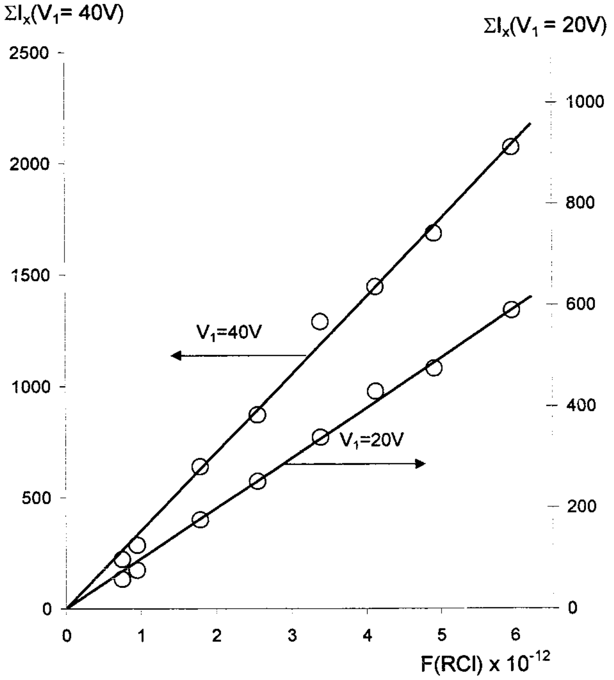

Figure 1. Sum of ion signals (in arbitrary units) of ethyl chloride (RCl) recorded from mass 25 to mass 66 at various specific flow rates (molecule/cm^3-s) of a 4.80% C_2H_5Cl/He mixture using 20 and 40 V ionization energies.

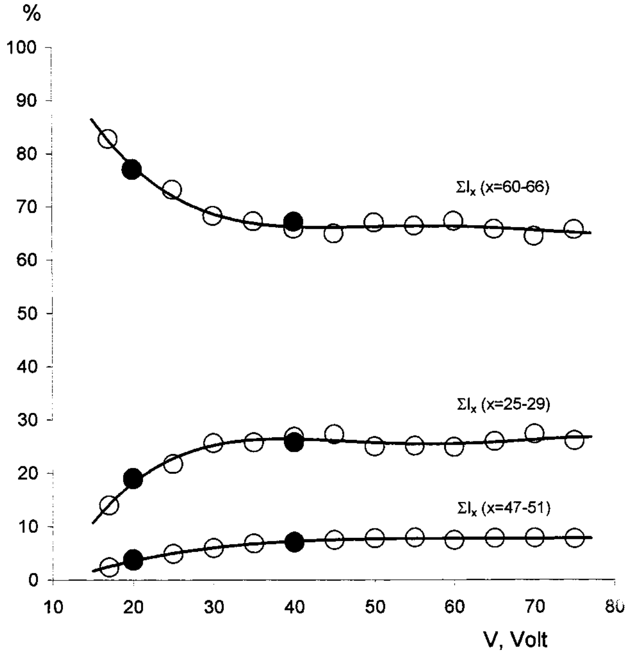

Figure 2. The three main group ion signal contributions (in percentage) of total ethyl chloride signals as a function of electron energy measured with 1.795 × 10^{12} molecule/(cm^3-s) specific flow rate of C_2H_5Cl. Solid circles represent average values of various flow rate measurements calculated from the data of Figure 1.

voltages used for kinetic measurements are as follows: For 40 eV, $\Sigma I_X(X = 25-29)$:$\Sigma I_X(X = 47-51)$:$\Sigma I_X(X = 60-66)$ = 26.70:7.03:66.27, and the individual mass intensity distributions (in percentage) within these groups are I_{66}:I_{65}:I_{64}:I_{63}:I_{62}:I_{61}:I_{60} = 22.45:2.31:**69.73**:2.88:1.12:0.93:0.58, I_{51}:I_{50}:I_{49}:I_{48}:I_{47} = 21.01: 2.65:**69.10**:5.22:1.90, and I_{29}:I_{28}:I_{27}:I_{26}:I_{25} = **34.51**:29.56:8.47: 0.56 (with the largest peaks in boldface). For 20 eV, $\Sigma I_X(X = 27-29)$:$\Sigma I_X(X = 47-51)$:$\Sigma I_X(X = 62-66)$ = 19.43:3.70:76.87, and the individual mass intensity distributions are I_{66}:I_{65}:I_{64}:I_{63}:I_{62} = 23.4:2.02:**72.69**:1.88:0.37, I_{51}:I_{50}:I_{49}:I_{48}:I_{47} = 22.85:2.34: **70.09**:4.00:0.72, and I_{29}:I_{28}:I_{27} = **49.38**:43.54:7.08 (with the largest peaks in boldface).

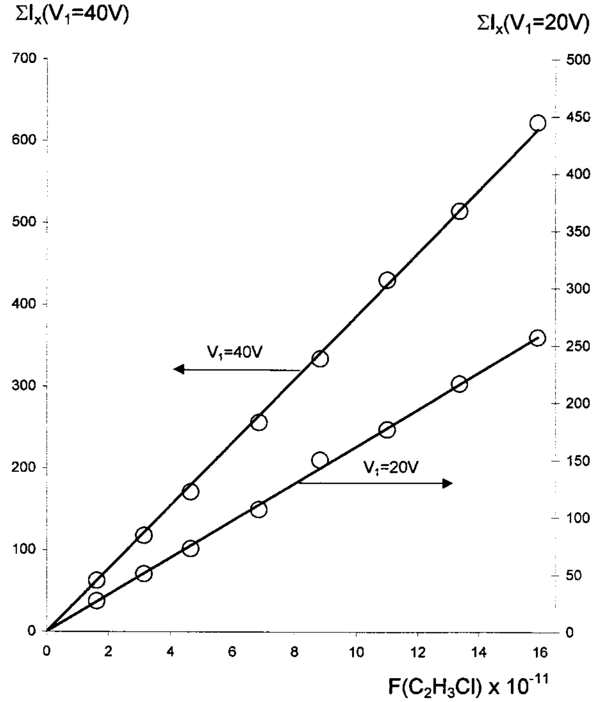

Figure 3. Sum of mass signals of vinyl chloride recorded from mass 25 to mass 64 at various specific flow rates of 4.84% C_2H_3Cl/He mixture using 20 and 40 V ionization energies.

There are no measurable signal intensities over the background values between these groups. The empty mass range between mass 35 and 39 indicates that no ionized fragment species (Cl, HCl) are found at up to 40 V electron energy. This finding simplifies the accurate measurement of Cl and HCl concentrations because they are free from fragment interference. The analysis also reveals that our C_2H_5Cl/He mixture is free from C_2H_6 contamination (no mass 30 signal). Mass signal I_{66}, the ^{37}Cl isotope of C_2H_5Cl, was chosen for the ethyl chloride concentration measurement. It is a compromise on sensitivity for a direct, fragment-interference-free C_2H_5Cl measurement. Its cross-section efficiency can be easily obtained from the signal intensity distributions described as $\alpha_{66} = 0.6627 \times 0.2245 \times \alpha_\Sigma(V = 40\text{ V}) = 5.249 \times 10^{-11}$ and $0.7687 \times 0.2304 \times \alpha_\Sigma(V = 20\text{ V}) = 1.787 \times 10^{-11}$. The increase in (the generally small) mass 65 signal intensity due to reactions is then a direct measure of the C_2H_4Cl radical concentration. The use of isotope mass signal intensities is the most straightforward mass spectral analysis of C_2H_5Cl and C_2H_4Cl concentrations compared with multistep corrections for fragment contributions to resolve the signal intensities of masses 64 and 63.

The fifth component of the reaction system is vinyl chloride formed in both reactions 2 and 3. A calibration procedure, similar to that of C_2H_5Cl, was carried out for C_2H_3Cl mass spectrometry using a 4.84% C_2H_3Cl/He gas mixture and recording the signal intensities in the mass range from 25 to 64. The total mass signal intensity versus the C_2H_3Cl specific flow rate is presented in Figure 3. The slopes corresponding to the cross-section efficiencies are $\alpha_\Sigma = (3.911 \pm 0.038) \times 10^{-10}$ with 40 V and $(1.624 \pm 0.022) \times 10^{-10}$ with 20 V electron energies. The fragment signals are found in two groups. The electron energy dependence of these group contributions is shown in Figure 4. The group distribution (in percentage) at the two electron voltages used for kinetic measurements are as

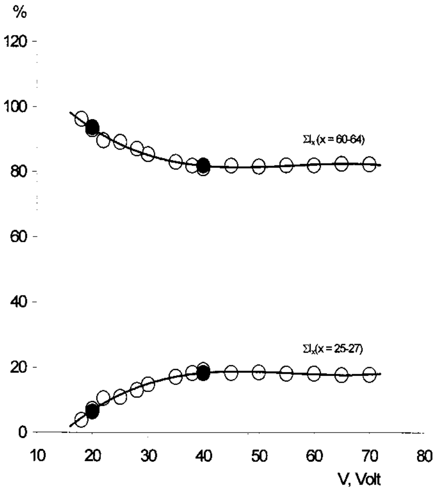

Figure 4. The two main group contributions (in percentage) of vinyl chloride fragmentation as a function of electron energy measured with 1.59×10^{12} molecule/(cm^3-s) specific flow rate of C_2H_3Cl. Solid circles represent average values of various flow rate measurements calculated from the data of Figure 3.

follows: For 40 eV, $\Sigma I_X(X = 25-27):\Sigma I_X(X = 60-64) = 18.21{:}81.79$, and the individual mass intensity distributions (in percentage) within these two groups are $I_{60}:I_{61}:I_{62}:I_{63}:I_{64} = 2.72{:}4.24{:}\mathbf{68.29}{:}2.73{:}22.24$ and $I_{25}:I_{26}:I_{27} = 5.60{:}21.88{:}\mathbf{72.62}$ (with the largest peaks in boldface). For 20 eV, $\Sigma I_X(X = 26-27):\Sigma I_X(X = 60-64) = 6.37{:}93.63$, and the individual mass intensity distributions are $I_{61}:I_{62}:I_{63}:I_{64} = 0.43{:}\mathbf{72.51}{:}1.83{:}25.23$ and $I_{26}:I_{27} = 2.75{:}\mathbf{97.25}$ (withe the largest peaks in boldface).

No measurable signal is found between these groups. Therefore, the mass spectral analysis of the Cl atom and HCl can be carried out with no signal interference from C_2H_3Cl fragments. However, the spectra of the two chlorohydrocarbons overlap in the mass range 60−64. They can be resolved for the $C_2H_3Cl + C_2H_5Cl$ composition using the distributions just presented to make appropriate corrections.

In the course of experimental measurements, the Cl_2 flow using a 5% Cl_2/He composition is started first through the microwave discharge inlet, and mass signal intensities of Cl_2 isotopes are repeatedly recorded. This measurement serves for the check of the mass spectral sensitivity using the known Cl_2 flow as standard. Then, the microwave generator is turned on and its power is adjusted to total dissociation of Cl_2, which is indicated by the disappearance of Cl_2 mass signals and their replacement by Cl atom and HCl signals. From the Cl/HCl signal intensity distribution measured with 20 V electron energy (column 2 of Table 1), the initial steady-state Cl concentration is calculated as $[Cl]_o = 2F(Cl_2)I_{Cl}/(I_{Cl} + I_{HCl})k_{eCl}$. These values are given in column 3 of Table 1. Afterward, the C_2H_5Cl flow is then started through the second inlet and gradually increased until a sizable decrease of Cl signal (accompanied by a balanced increase of HCl signal) is achieved. The new Cl and HCl signal intensities are repeatedly scanned and the Cl/HCl distribution as well as the Cl concentration are calculated (columns 5 and 6 of Table 1, respectively). The initial C_2H_5Cl concentration (column 4 of Table 1) is calculated from the flow of the C_2H_5Cl/He mixture. Then, the mass spectrometer is set to scan the mass range 60−66 repeatedly using both 20 and 40 V electron energies. The C_2H_5Cl concentration (column 7 of Table 1) is calculated from the average of mass 66 intensities measured at both voltages. Note that the Cl atom and HCl molecules have the same spectral sensitivities.[3]

Results

The overall mass analysis shows no measurable products outside those of reactions 1−3. When correcting the mass signal intensities of masses 60 and 61 for contributions from C_2H_5Cl and C_2H_3Cl fragmentation, they are reduced to near zero values. Also, no dichloro products of Cl addition to vinyl chloride, which would require effective third-body collisions to occur, are found in the mass range 90−100. These observations indicate that no further reaction of the Cl atom with vinyl chloride take place in our millitorr pressure system.

Application of steady-state conditions for that three-reaction system leads to kinetic equations similar to those we have derived for the Cl/C_2D_6 reaction system[16] earlier.

Combination of the steady-state kinetic equation for ethyl chloride (RCl) consumption and chloroethyl radical (R$^{\bullet}$Cl) formation defines the steady-state [R$^{\bullet}$Cl] concentration as

$$[R^{\bullet}Cl] = \frac{\mathbf{2}\Delta[RCl]k_{eRCl} - k_1[RCl][Cl]}{k_2[Cl] + k_{eR\bullet Cl}} \tag{6}$$

The radical concentration can also be derived from the consumption differences of reactants as

$$[R^{\bullet}Cl]k_{eR\bullet Cl} = 2\Delta[RCl]k_{eRCl} - \Delta[Cl]k_{eCl} \tag{6a}$$

where $\Delta[RCl] = [RCl]_o - [RCl]$ and $\Delta[Cl] = [Cl]_o - [Cl]$.

Substituting eq 6 into the steady-state kinetic equation for Cl atom consumption, the basic kinetic equation for combined Cl atom and RCl consumptions is obtained as

$$\frac{\Delta[Cl]}{[Cl]}k_{eCl} - \mathbf{2}f_2\frac{\Delta[RCl]}{[Cl]}k_{eRCl} = (\mathbf{1} - f_2)k_1[RCl] \tag{7}$$

where

$$f_2 = \frac{k_2[Cl]}{k_2[Cl] + k_{eR\bullet Cl}} \quad \text{and} \quad (\mathbf{1} - f_2) = \frac{\mathbf{1}}{\mathbf{1} + k_2[Cl]/k_{eR\bullet Cl}}$$

Because k_2 is not known yet, eq 7 is examined by linear regression analysis by floating k_2 around its expected value. The best solution of eq 7 is obtained with $k_2 = 1.18 \times 10^{-11}$ cm^3/(molecule-s) as shown in Figure 5, where the slope is equal to

TABLE 1: Initial and Final Steady-State Concentrations[a] of Reactants and Products Formed in Reactions 1−3

no.	$\frac{I^o_{Cl}}{I^o_{Cl} + I^o_{HCl}} \times 10^2$	$[Cl]_o$	$[C_2H_5Cl]_o$	$\frac{I_{Cl}}{I_{Cl} + I_{HCl}} \times 10^2$	[Cl]	$[C_2H_5Cl]$	$[C_2H_4Cl]$[b]	$[C_2H_3Cl]$[c]
1	45.6[d]	9.23	7.64	14.0	2.83	2.70	1.22	3.66
2	49.4[d]	9.99	9.93	11.8	2.38	3.96	1.65	4.25
3	52.8[d]	10.68	11.36	11.1	2.25	4.74	1.83	4.70
4	52.8[d]	10.68	14.51	8.2	1.65	7.23	2.37	4.85
5	34.8[d]	7.05	13.35	5.2	1.05	8.16	2.12	2.94

[a] All concentrations are in units of 10^{11} particles/cm^3. [b] Calculated according to eq 6. [c] Calculated according to eqs 10 and 10a. [d] Spectral sensitivities of Cl and HCl are the same.

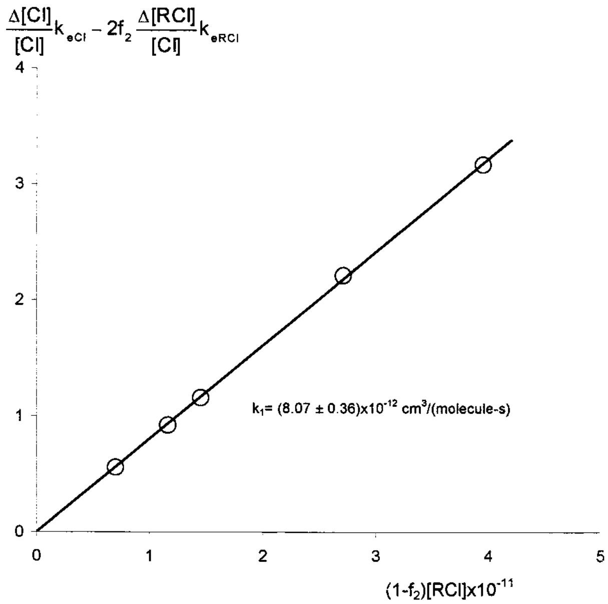

Figure 5. Relative consumption rate of reactants as a function of reduced ethyl chloride (RCl) concentration in the Cl/RCl two-component system plotted according to eq 7. The slope gives k_1 directly.

the rate constant $k_1 = (8.07 \pm 0.36) \times 10^{-12}$ cm^3/(molecule-s). With the knowledge of these rate constants, the R$^\bullet$Cl radical concentrations for each experimental run can also be calculated according to eq 6. These calculated values are given in column 8 of Table 1.

Knowing k_1 and the radical concentrations, the disproportionation rate constant of reaction 2 can be rechecked and its scatter calculated according to the kinetic equation

$$k_2[Cl] = \frac{\Delta[Cl]k_{eCl} - k_1[RCl][Cl]}{[R^\bullet Cl]} \qquad (8)$$

that is derived from the steady-state condition of Cl atom consumption. The plot of data according to eq 8 is presented in Figure 6 where the slope gives the rate constant of reaction 2 directly as $k_2 = (1.18 \pm 0.06) \times 10^{-11}$ cm^3/(molecule-s).

Applying the steady-state conditions for ethyl chloride consumption, a kinetic equation for the radical disproportionation is obtained as

$$k_3[R^\bullet Cl]^2 = k_1[RCl][Cl] - \Delta[RCl]k_{eRCl} \qquad (9)$$

The plot of data according to eq 9 is shown in Figure 7 where the slope gives $k_3 = (1.83 \pm 0.15) \times 10^{-12}$ cm^3/(molecule-s).

Because of the C_2H_4Cl radical formation, a relative increase of mass 65 intensity (and also of mass 63) is observed in each run. The increase in the I_{65} intensity can be calculated by subtracting the fragmentation contribution of C_2H_5Cl (mass 66) from the measured I_{65} value: $\Delta I_{65} = I_{65} - \alpha_{66}I_{66}/\alpha_{65}$. These excess intensities are proportional to the chemically generated F(R$^\bullet$Cl) flow in each run, from which the mass spectral efficiency for C_2H_4Cl can be recovered as $\alpha_{R^\bullet Cl} = (0.711 \pm 0.055) \times 10^{-11}$ with 40 V and $(0.298 \pm 0.034) \times 10^{-11}$ with 20 V electron energy.

Vinyl chloride (VCl) is produced in both reactions 2 and 3. Its specific flux can be obtained either from the combination of the steady-state kinetics for Cl and C_2H_5Cl consumptions and C_2H_3Cl formation as

$$[VCl]k_{eVCl} = \Delta[Cl]k_{eCl} - \Delta[RCl]k_{eRCl} \qquad (10)$$

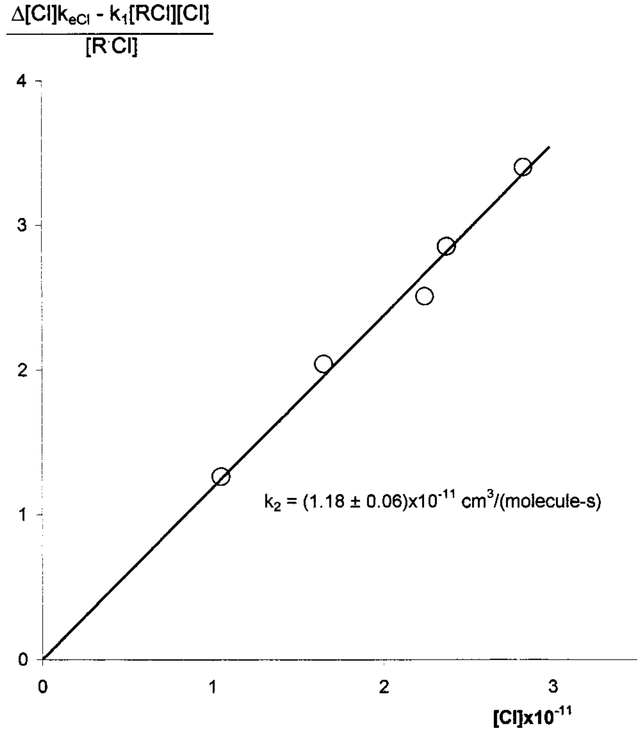

Figure 6. Cl + chloroethyl radical (R$^\bullet$Cl) disproportionation rate (reaction 2) in the Cl/RCl two-component system plotted according to eq 8. The slope gives k_2 directly.

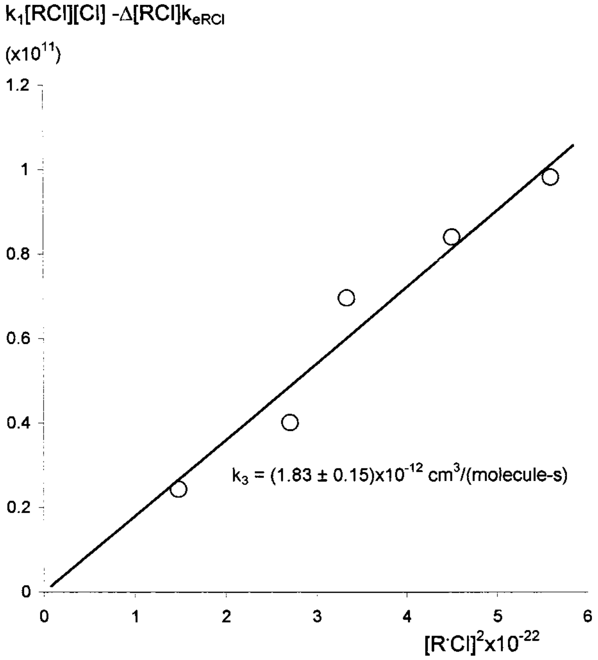

Figure 7. The chloroethyl radical (R$^\bullet$Cl) disproportionation rate (reaction 3) in the Cl/RCl two-component system plotted according to eq 9. The slope gives k_3 directly.

or from the flow balance of chlorocarbon species as

$$[VCl]k_{eVCl} = \Delta[RCl]k_{eRCl} - [R^\bullet Cl]k_{eR^\bullet Cl} \qquad (10a)$$

The vinyl chloride concentration values calculated according to eq 10 are given in column 9 of Table 1.

The appearance of the vinyl chloride product is also indicated by the increase of mass 62 intensity in the mass spectrum. Direct spectrometric measurement would, however, require a correction of I_{62} for the C_2H_5Cl contribution, which can be done by using the C_2H_5Cl fragment distribution pattern, and a second correction for the C_2H_4Cl radical fragment contribution, which is not known. Without that latter correction, the $\Delta I_{62} = \alpha_{VCl}F(VCl)$ function gives values for α_{VCl} that are 15% higher with 40 V and 10% higher with 20 V electron energies than the mass spectral calibration values for vinyl chloride for mass 62 intensity. These deviations point to an appreciable contribution of the radical fragmentation to mass 62.

Although reaction 5 is not a constituent of our kinetic system, we have checked its controversial influence in the flash systems[11−14] by introducing a 10% Cl_2/He composition flow into the last run (no. 5) of Table 1 through a third inlet of the reactor. High flow of Cl_2 corresponding to $[Cl_2]_o = 2.43 \times 10^{12}$ molecule/cm^3 was needed to cause observable $C_2H_4Cl_2$ product signals at masses 98 and 83, whereas the chlorine concentration dropped to $[Cl_2] = (2.35 \pm 0.06) \times 10^{12}$ molecule/cm^3 only. The measured new steady-state concentrations of other components are: $[C_2H_5Cl] = 7.21 \times 10^{11}$, $[C_2H_4Cl] = 2.00 \times 10^{11}$, $[Cl] = 1.13 \times 10^{11}$, and $[HCl] = (2.02 \pm 0.02) \times 10^{12}$ molecule/cm^3. Calculating the rate constant from the Cl_2 consumption kinetics as $k_5 = \Delta[Cl_2]k_{eCl}/[Cl_2][R^{\bullet}Cl]$, $k_5 = (1.9 \pm 1.4) \times 10^{-13}$ cm^3/(molecule-s) is obtained. This rate constant can also be obtained from the steady-state consumption of Cl atom and HCl formation kinetics as $k_5 = -(\Delta[Cl]k_{eCl} + \Delta[HCl]k_{eHCl})/[Cl_2][R^{\bullet}Cl]$, which gives $k_5 = (1.4 \pm 0.7) \times 10^{-13}$ cm^3/molecule-s), where $\Delta[HCl] = [HCl]_o - [HCl]$ is a negative term. An average of the two measurements gives $(1.7 \pm 1.0) \times 10^{-13}$ cm^3/(molecule-s).

Discussion

The detailed kinetic investigation of the $Cl + C_2H_5Cl$ reaction in the VLPR system discloses that the overall mechanism comprises three elementary steps, reactions 1−3. The overall reactant and product analysis allows the determination of rate constants for each step.

The measured rate constant k_1 is in excellent agreement with the value reported by Wine et al.,[11] and a measurement of reaction 5 shows it makes no significant contribution to the kinetic measurement in the Cl_2 flash system. Because of small concentration changes in our single control measurement in the three-component system, the scatter of k_5 is large, but it is well within the range estimated by Wine et al.[11] Our value of k_1 is also in good agreement with the results of relative rate measurements[5,7] and of the flash/IR spectrometry technique[13] at low C_2H_5Cl concentration measurements, where reactions 4 and 5 have only a small effect.

Substitution of an H atom by Cl in ethane reduces the molecular reactivity of C_2H_5Cl to Cl metathesis in comparison with the reactivity of C_2H_6 by a factor 7.6 on molecular basis, or by a factor of 6.4 on a per H atom basis ($5k_{EtH}/6k_1 = 6.4$), despite reaction 1 being 3.4 kcal/mol more exothermic than the $C_2H_6 + Cl$ reaction. At the same time, the Cl atom substitution weakens the C−H bond strength of the $-CH_2$ group by ~1 kcal/mol, but makes no bond energy change for the $-CH_3$ group. The change in the reactivity pattern is even more explicit when the group reactivities are compared. The reactivity of the $-CH_3$ group in C_2H_5Cl is reduced by a factor of 21 ($0.5k_{EtH}/0.18k_1 = 21.2$). A comparative decrease of the $-CH_2$ group reactivity can be derived from the rate constant of $(CH_3)_2CH_2 + Cl$ reaction, where $k_{PrH} = (1.6 \pm 0.14) \times 10^{-10}$ cm^3/(molecule-s) at room temperature.[17] The partial reactivity of that $-CH_2$ group is reduced by a factor of 15 [$(k_{PrH} - k_{EtH})/0.82k_1 = 15.1$] by replacing one $-CH_3$ group of propane by a Cl atom.

These reactivity changes are reflected in the Arrhenius parameters[11] for reaction 1, where the A_1 is decreased by a factor of 3.5 and E_1 is increased by 0.45 kcal/mol in comparison with the Arrhenius parameters for the $Cl + C_2H_6$ reaction.[3] Such changes can only be interpreted on the basis of the polar character of the TS complex with dipole−dipole repulsion in the transition state.

Metathesis reactions between radicals and molecules are most easily interpreted as an electrophilic attack of the radical on the electrons of the donor bond in the molecule.[18] In the case of Cl attack on ethane, the TS is pictured as a 3-electron system:

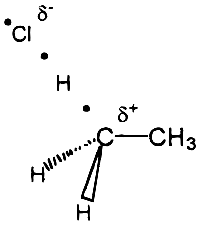

with a partial negative charge on Cl and a partial positive charge on the attacked C. In the adjacent $-CH_3$ group, carbon is electronegative relative to H and thus favors an adjacent positive charge. The substitution of H by an electronegative Cl atom in this methyl group changes its polarity unfavorably. Note that this is also true if the substitution is in the α-position:

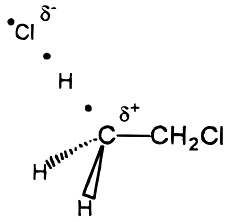

β

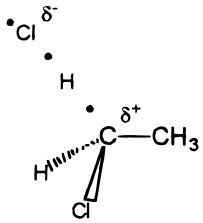

α

The ground state of C_2H_6 has an opposing partial negative charge on the C atom due to its greater electronegativity relative to H. By way of contrast, the ground state of C_2H_5X has some positive charge on the substituted C atom and some negative charge on the other C atom, which is a more stable configuration than in C_2H_6.

This model suggests that the rate constant should decrease with increasing electronegativity of the halogen substituent of reactant in the reaction

$$Cl + C_2H_5X \rightarrow HCl + C_2H_4X \qquad (11)$$

where X = H, Br, Cl, or F atom. Rate constants for reactions with Br[19] and F atom[20] substituted in C_2H_5X are also known: $k_{EtBr} = (14 \pm 4) \times 10^{-12}$ and $k_{EtF} = (7.55 \pm 2.14) \times 10^{-13}$ cm^3/(molecule-s). Plotting ln k_{EtX} versus the electronegativity values (χ_P) of halogen or H atom substituents given on the Pauling scale[21] results in a good linear relationship, as shown in Figure 8. Figure 8 indicates that the main driving force in reaction 11 is rather proportional to the dipole moment of the C−X heteroatomic bond than to the bond strength of the attacked C−H bond. This is why the Evans−Polanyi relationship does not hold for reactions of halogenated compounds.[22] Most of other electronegativity scales of X atoms, like the recently introduced covalent potential,[23] also give formal linear relationships similar to that of Figure 8. Reactivity of polyhalogenated

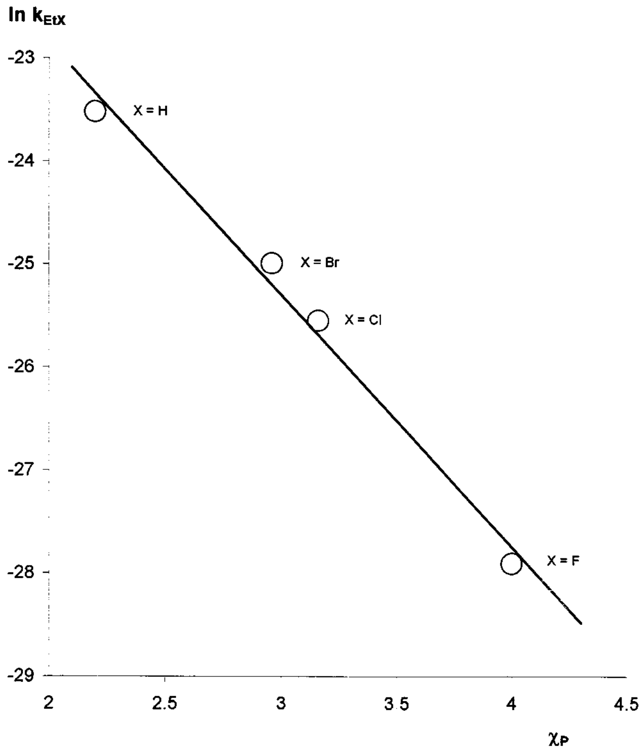

Figure 8. The activation free energy change of reaction 11 as a function of electronegativities of X substituents on the Pauling scale.

hydrocarbons is a more complex problem where internal contributions from local dipoles have to be taken into account.[20,24]

Reaction 2 is an important step of the overall reaction mechanism because it is responsible for 24−31% of the total Cl atom consumption. The measured rate constant is about the same as for the similar C_2H_5 + Cl or Br reactions reported earlier.[3,25] This reaction proceeds via a recombination to form a vibrationally excited singlet $[C_2H_4Cl_2]^*$, which is the rate-determining step, followed by a rapid four-center elimination to produce HCl. Detailed analysis of such atom−radical disproportionation is described in our earlier work.[26]

The direct mass spectrometric measurement of the C_2H_4Cl radical decay in our VLPR system allows us to obtain the radical−radical disproportionation rate constant k_3 without any interference from other radical−radical decay processes such as recombination at such low (mTorr) pressures. No mass signal of a recombination product was ever found in the mass range 125−128. The measured value of k_3 is ~10% lower than that for C_2H_5 radical disproportionation.[3] Only measurements for the disproportionation−recombination ratios (k_d/k_c) for C_2H_4-Cl radicals are known. They have been studied between 3 and 760 Torr pressures by the reaction scheme:

$$2C_2H_4Cl \rightarrow C_2H_5Cl + C_2H_3Cl \qquad (12a)$$

$$\rightarrow C_2H_4Cl_2 + C_2H_4 \qquad (12b)$$

$$\rightarrow C_4H_8Cl_2 \qquad (12c)$$

Rate constant ratios for reactions 12a and 12c are reported as 0.05,[27] 0.1,[28] 0.21,[29] and 0.36,[30] whereas the ratios for reactions 12b and 12c are 0.1,[28] 0.21,[29] and 0.09.[30] Concerning the disproportionation variant 12b, we could find neither traces of dichloroethane in the mass range 98−100, nor any measurable increase of mass 28 signal intensity over that from the C_2H_5Cl fragmentation. The reported k_d/k_r ratios (k_{12a}/k_{12c}) are not precise enough to calculate a reliable k_r value using our measured rate constant k_3, but suggest it is in the range of 6×10^{-12} to 42×10^{-12} cm^3/(molecule-s).

Conclusions

The VLPR system offers a well-controlled experimental technique for the accurate kinetic investigation of the multistep chemical process Cl + C_2H_5Cl at millitorr pressures. Detailed mass analysis of reactants and products using sensitive mass spectrometric measurements discloses that the overall mechanism is comprised of three elementary steps, reactions 1−3, which account for ~98% mass balance of chemical changes in the system. Rate constants for each elementary step can be calculated from the analytical data.

We find $k_1 = (8.07 \pm 0.36) \times 10^{-12}$ cm^3/(molecule-s), which is in excellent agreement with the value reported from the Cl_2 flash/Cl resonance fluorescence study.[11] It is also in good agreement with the results of relative rate[5,7] and Cl_2 flash/IR spectrometry of HCl product measurements[13] The decrease in the molecular reactivity of C_2H_5Cl compared with that of C_2H_6 in H abstraction reaction with Cl atom correlates well with the electronegativity of the Cl substituent arising from a dipole−dipole repulsion in transition state. Such an effect of halogen substituents in C_2H_5X (X = H, Br, Cl, F) is shown in Figure 8.

The measured rate constant for reaction 2 is $k_2 = (1.18 \pm 0.06) \times 10^{-11}$ cm^3/(molecule-s), which is about the same as obtained earlier for C_2H_5 + Cl or Br reactions.[3,25] This value is consistent with the proposed mechanism of atom + radical disproportionation.[26] Most striking is the absence of any radical recombination products. Measurements for radical−radical disproportionation rate gives $k_3 = (1.83 \pm 0.15) \times 10^{-12}$ cm^3/(molecule-s), which is slightly less than that measured for the $2C_2H_5$ disproportionation.[3] A few measurements of the C_2H_4-Cl reaction with Cl_2 give a value of $k_5 = (1.7 \pm 1.0) \times 10^{-13}$ cm^3/(molecule-s) for the rate constant.

Acknowledgment. Acknowledgment is made to the donors of the Petroleum Research Fund, administered by the American Chemical Society, for the support of this research. We are also indebted to Prof. Irving S. Reed of the Electrical Engineering Department at USC for a grant in support of the present work.

References and Notes

(1) Poutsma, M. L. *Halogenation* in *Free Radicals*; Kochi, J. K., Ed.; Wiley: New York, 1973; Vol. 2, Chapter 15.

(2) Pritchard, H. O.; Pyke, J. B.; Trotman-Dickenson, A. F. *J. Am. Chem. Soc.* **1955**, *77*, 2629.

(3) Dobis, O.; Benson, S. W. *J. Am. Chem. Soc.* **1990**, *112*, 1023; Dobis, O.; Benson, S. W. *J. Am. Chem. Soc.* **1991**, *113*, 6377.

(4) Wallington, T. J.; Andino, J. M.; Lorkovic, I. M.; Kaiser, E. W. *J. Phys. Chem.* **1990**, *94*, 3644, Wallington, T. J.; Andino, J. M.; Ball, J. C.; Japar, S. M. *J. Atmos. Chem.* **1990**, *10*, 301; Wallington, T. J.; Skewes, L. M.; Siegl, W. O. *J. Phys. Chem.* **1989**, *93*, 3649.

(5) Shi, J.; Wallingto, T. J.; Kaiser, E. W. *J. Phys. Chem.* **1993**, *97*, 6184.

(6) Tschuikow-Roux, E.; Yano, T.; Niedzielski, J. *J. Phys. Chem.* **1984**, *88*, 1408.

(7) Niedzielski, J.; Tschuikow-Roux, E.; Yano, T. *Int. J. Chem. Kinet.* **1984**, *16*, 621; Tschuikow-Roux, E.; Niedzielski, J.; Faraji, F. *Can. J. Chem.* **1985**, *63*, 1093.

(8) Kaiser, E. W.; Wallington, T. J.; Hurley, M. D. *Int. J. Chem. Kinet.* **1995**, *27*, 205.

(9) Dobis, O.; Benson, S. W. *Int. J. Chem. Kinet.* **1987**, *19*, 691.

(10) Miyokawa, K.; Tschuikow-Roux, E. *J. Phys. Chem.* **1990**, *94*, 715; Tschuikow-Roux, E.; Paddison, S. *Int. J. Chem. Kinet.* **1987**, *19*, 15.

(11) Wine, P. H.; Semmes, D. H. *J. Phys. Chem.* **1983**, *87*, 3572.

(12) Kaiser, E. W.; Rimai, L.; Schwab, E.; Lim, E. C. *J. Phys. Chem.* **1992**, *96*, 303; Kaiser, E. W.; Wallingto, T. J. *J. Phys. Chem.* **1995**, *99*, 8669.

(13) Mariq, M. M.; Shi, J.; Szente, J. J.; Rimai, L.; Kaiser, E. W. *J. Phys. Chem.* **1993**, *97*, 9686.

(14) Kaiser, E. W.; Wallington, T. J.; Andino, J. M. *Chem. Phys. Lett.* **1990**, *168*, 309.

(15) Knyazev, V. D.; Bencsura, A.; Dubinsky, I. A.; Melius, C. F.; Senkan, S. M. *J. Phys. Chem.* **1995**, *99*, 230.

(16) Dobis, O.; Benson, S. W.; Mitchell, T. J. *J. Phys. Chem.* **1994**, *98*, 12284.

(17) Lewis, R. S.; Sander, S. P.; Wagner, S.; Watson, R. T. *J. Phys. Chem.* **1980**, *84*, 2009.

(18) Benson, S. W. *Thermochemical Kinetics*, 2nd ed.; Wiley: New York, 1976; p 194.

(19) Donaghy, T.; Shanahan, I.; Hande, M.; Fitzpatrick, S. *Int. J. Chem. Kinet.* **1993**, *25*, 284.

(20) Tschuikow-Roux, E.; Yano, T.; Niedzielski, J. *J. Chem. Phys.* **1985**, *82*, 65.

(21) Allred, A. L. *J. Inorg. Nucl. Chem.* **1961**, *17*, 215.

(22) Senkan, S. M.; Quam, D. *J. Phys. Chem.* **1992**, *96*, 10837.

(23) Luo, Y. R.; Benson, S. W. *Acc. Chem. Res.* **1992**, *25*, 375.

(24) Moore, L. O.; Rectenwald, C. E.; Clark, J. W. *Int. J. Chem. Kinet.* **1972**, *4*, 331.

(25) Dobis, O.; Benson, S. W. *J. Phys. Chem. A* **1997**, *101*, 6030.

(26) Benson, S. W.; Dobis, O. *J. Phys. Chem. A* **1998**, *102*, 5175.

(27) Roquitte, B. C.; Wijnen, M. H. *J. Am. Chem. Soc.* **1963**, *85*, 2053.

(28) Roquitte, B. C.; Wijnen, M. H. *J. Chem. Phys.* **1963**, *38*, 4.

(29) Dees, K.; Sester, D. W.; Clark, W. G. *J. Phys. Chem.* **1971**, *75*, 2231.

(30) Heicklen, J. *J. Am. Chem. Soc.* **1965**, *87*, 445.